BIOSCIENCES BIOTECHNOLOGY RESEARCH ASIA, September 2022. Vol. **19**(3), p. 657-670

Individual and Synergistic Potential of Bioactive Compounds from Chrysopogon Zizanioides Against Main-Protease of SARS-Cov-2 using Computational Approach

Venkataraghavan Ragunathan[1], Thiruchelvi Ramakrishnan[2,3]* and Rajnish Narayanan[3]

[1]Department of Chemical Engineering, Alagappa College of Technology, Anna University, Chennai 600025, Tamil Nadu, India.
[2]Department of Bio-Engineering, School of Engineering, Vels Institute of Science Technology and Advanced Studies, Pallavaram, Chennai 600117, Tamil Nadu, India.
[3]Department of Genetic Engineering, SRM Institute of Science and Technology, Kattankulathur, 603203, Tamil Nadu, India.
*Corresponding Author E-mail: thiruchelvir13@gmail.com

http://dx.doi.org/10.13005/bbra/3018

(Received: 26 March 2022; accepted: 08 July 2022)

This study presents the anti-COVID potential of bioactive compounds from Chrysopogon zizanioides thorough in-silico molecular docking approach using AutoDock Vina software. As of our knowledge, the antiviral potential of all its bioactive compounds and their synergistic potentials against SARS-CoV-2 main-protease is not reported earlier. The results were promising with ß-Sitosterol (?G = -7.5 kcal/mol; Ki = 3.13 μM); Campesterol (?G = -7.4 kcal/mol; Ki = 3.71 μM); Stigmast-4-en-3-one (?G = -7.3 kcal/mol; Ki = 4.39 μM) forming non-covalent interactions with the amino acids in the active site of Mpro causing inhibition. The synergistic potential of compounds showed a significant sign of inhibition against Mpro with -7.9 kcal/mol with the sequential combination of ß-Sitosterol; Campesterol; Stigmast-4-en-3-one. The docking protocol validation was performed by re-docking and superimposing co-crystallized ligand, and interactions visualized using Discovery Studio 2020. Moreover, all the compounds satisfied Lipinski's oral drug-likeliness properties to be used and oral drug. These bioactive compounds of Chrysopogon zizanioides showed low binding energies against SARS-CoV-2 Mpro which proved their anti-COVID potential. Thus, by incorporating Chrysopogon zizanioides for consumption in daily life, it is very likely that one can get rid of COVID-19.

Keywords: AutoDock Vina; Chrysopogon zizanioides; COVID-19; Main-protease; SARS-CoV-2.

Coronavirus disease 2019, a pandemic caused by the deadly new strain of virus severe acquired respiratory syndrome coronavirus-2 (SARS-CoV-2) identified in December 2019 in China, has claimed millions of lives throughout the globe in several countries [1]. A total of 500 million people were affected and 6 million people were claimed globally due to COVID-19 infection as of now since its outbreak and still counting. Several symptoms from mild to severe have been reported due to the viral infection, include cold, high fever, nausea, vomit, cough, shortness of breath, loss of

*Corresponding author E-mail:

taste, and smell persisting over five days. There has been no cure till now [2]; however, several preventive medicines such as vaccines are in the process of administration to develop immunity against the virus. In addition, several drugs like remdesivir, hydroxychloroquine, ivermectin, lopinavir, darunavir, etc. have been repurposed as a drug of choice to combat the disease. The mentioned drugs are used as temporary 'drug of choice' to combat the infection, however, no proven treatment is available till now. This brings us in search of alternate treatment from natural sources, bringing to this research work, which is the need of the hour. One of the most important target sites in SARS-CoV-2 is the main-protease causing the proteolytic processing of polyproteins to non-structural proteins responsible for viral replication and transcription [3]. The 3C-like proteinase from SARS-CoV-2 has three domains with 306 amino acids and a molecular weight of 34.29 kDa tightly bound with X77 ligand in its active site. The main-protease is involved in the replication and transcription of the virus by forming functional proteins. 3C-like proteinase is catalytically active at amino acid residues HIS41 and CYS145 in the active center of the SARS-CoV-2 main-protease. Therefore, inhibiting the active site is an excellent solution to stop the activity and virulence of the virus.

The use of herbal and ayurvedic medicines have gained pace in recent times for treating viral disease. Traditional herbal formulations of bioactive compounds are of great interest even in the present world due to their high efficiency to cure and minimal side effects [4]. Bioactive constituents from essential oils of *Chrysopogon zizanioides* is a cocktail of sesquiterpene alcohols and hydrocarbons and are widely used as a promising medicine to cure various ailments [5]. *Chrysopogon zizanioides*, commonly known as 'vetiver', is one of the most widely used phytoconstituents in Indian medicines since ancient times due to its antioxidant, anti-inflammatory, antiviral, antimicrobial, anti-tubercular, and anticancer properties [6]. In addition, the metabolites from leaves and roots are commonly used to cure rheumatic diseases and gastritis [7]. The present research work retrieved the bioactive compounds from *Chrysopogon zizanioides*, and their antiviral potential was studied. The volatile essential oils in *Chrysopogon zizanioides* have an immense flavor and aroma and are used widely uses as an additive to impart flavor to water. Only a handful of studies have reported the anti-COVID potential of *Chrysopogon zizanioides* targeting the spike protein and ACE2 receptor; however, there has been no research on their synergistic potential against main-protease. The computational tools are rapid, comprehensive, reproducible, robust, and accurate in prediction; thus, their usage is essential in every sector. Molecular docking is one of the most important and supportive tools to study the interaction between the protein and ligand at the atomic level using various algorithms and programs to discover or invent drugs specific to the target [8]. Therefore, the present research aims to fill the gap by exploring the individual and synergistic antiviral property of *Chrysopogon zizanioides* against the COVID-19 M^{pro} using *in-silico* bioinformatics tools. It is very essential and immediate measures need to be taken to contain the spread of COVID-19 infection to save the lives of people as currently repurposed drugs and treatment strategies have shown poor efficiency against the viral infection. The toxicity properties of bioactive compounds are also discussed in the study. The workflow of the research is shown in Figure 1.

MATERIALS AND METHODS

Computer parameters

The system parameters used in the present study for molecular docking were as follows, RAM: 16 GB; Operating system and type: Windows 10, 64 bit, x64-based processor; Processor: Intel(R) Core(TM) i5-10210U.

Retrieval of bioactive compounds from literature and preparation

A total of 91 bioactive compounds from *Chrysopogon zizanioides* were obtained from literature sources [9,10]. The bioactive compounds were subjected to Lipinski's filter to screen the compounds that satisfy oral drug-likeliness properties [11]. The compounds that satisfied Lipinski's rule were then retrieved from the PubChem database in SDF format and converted into PDBQT (Protein data bank partial charge and atom type) format using Open Babel GUI software [12] before docking. The compounds were then energy minimized for 200 iterations to correct and optimize the geometry, which was accomplished

using the Hartree-Fock algorithm of Quantum mechanics/Molecular mechanics (QM/MM) force field [13,14].

Protein preparation

The three-dimensional structure of SARS-CoV-2 M^{pro} (PDB Id: 6W63) was retrieved from the protein data bank in PDB format. The geometry was optimized using the SwissPDB viewer [15] and GROMOS_96 force field [16] to eliminate bad clashes and correct the bond angles. The heteroatoms like water molecules and ligand were removed, polar hydrogens, Gasteiger, and Kollman charges were added using AutoDockTools-1.5.6 and used for molecular docking.

Predicting the ligand-binding site

The ligand-binding site of M^{pro} was predicted using MetaPocket 2.0 webserver [17] to direct the ligands for site-directed docking. Once the amino acids present in the ligand-binding site were identified, the grid box was fixed to enclose the total amino acids present in ligand-binding site and were found to be X center = -20.774; Y center = 16.188; Z center = -31.912 and size X = 70; Y = 82; Z = 84 with a grid spacing of 0.375 Å. The grid box size and dimensions set were according to Pant et al. [18].

Molecular docking of protein and bioactive compounds using AutoDock Vina

Molecular docking using AutoDock Vina [19] was performed for 100 Genetic Algorithm runs with exhaustiveness of 4; Population size 150. The responses were studied in terms of binding energy where the compounds with low binding energy have the highest inhibition potential and vice-versa. The software calculates the free binding energy using the equation proposed by Morris et al. [20].

Each compound's inhibition constant (Ki) value was calculated using the following equation (1).

$$Ki = e^{\frac{\Delta G}{RT}} \quad ...(1)$$

Where ÄG is the intermolecular free binding energy; R is the gas constant; T is the temperature (298 K). Sequential synergistic docking was performed to study the augmented inhibition upon docking multiple compounds to the same enzyme. The top-ranked free binding energy compound-Mpro complex was sequentially docked with successive bioactive compounds using the same procedure to increase free binding energy, and their potentials were studied. According to C et al. [21], the molecular docking procedure was substantiated by re-docking the X77 ligand that is co-crystallized with M^{pro} using the above-set docking parameters and procedure. The re-docked X77-M^{pro} complex was then superimposed onto the actual native co-crystallized M^{pro}. A low root means square deviation (RMSD < 2 Å) value denotes the validity of the docking procedure. The bound interactions between the compounds and M^{pro} were elucidated using PyMOL 2.3 and Discovery studio 2020 software. The toxicity properties of the top 10 low binding energy compounds were predicted using SwissADME and admetSAR webservers [22,23].

RESULTS AND DISCUSSION

Docking bioactive compounds against M^{pro} using AutoDock Vina

The use of natural bioactive compounds has shown promising results by inhibiting the main-protease from the literature [24–26]. All compounds used in the present study fulfilled Lipinski's rule of five. The molecular docking results (Table 1) in the present study showed significant inhibition (ÄG = -7.5 to -4.0 kcal/mol).

The lower binding energy of protein-ligand complex denotes a greater inhibition property. Of the 91 bioactive compounds from *Chrysopogon zizanioides*, the top five compounds (Figure 2) with low free binding energy obtained from molecular docking were reported in table 2.

The supramolecular bonding interactions of the top five bioactive compounds with M^{pro} were shown in Figure 3 (a) to (e).

The phytosterol â-Sitosterol was found to be the best potential inhibitor of M^{pro} with a free binding energy of -7.5 kcal/mol (Ki = 3.13 µM) that interacted with the amino acids ARG188, ASN142, ASP187, CYS44, GLN189, GLN192, GLU166, GLY143, HIS41, MET49, MET165, THR25, THR26, THR190, and TYR54 in the active site of the enzyme (Figure 4).

Dimensional cartoon image

This binding energy was accomplished by forming non-covalent intermolecular bonding like van der Waals, carbon-hydrogen, ð-alkyl, alkyl, and ð-sigma bonds. The low binding

energy is accomplished due to the hydrophobic nature of â-Sitosterol, causing a low entropy (ÄS) change in the enzyme's surface, causing fluid displacement. The molecular solvent accessibility for the interaction was 3555 Å. Campesterol ranked second with the binding energy of -7.4 kcal/mol (Ki = 3.71 µM) binding with ARG188, ASN142, ASN187, CYS44, GLN189, GLU166, HIS41,

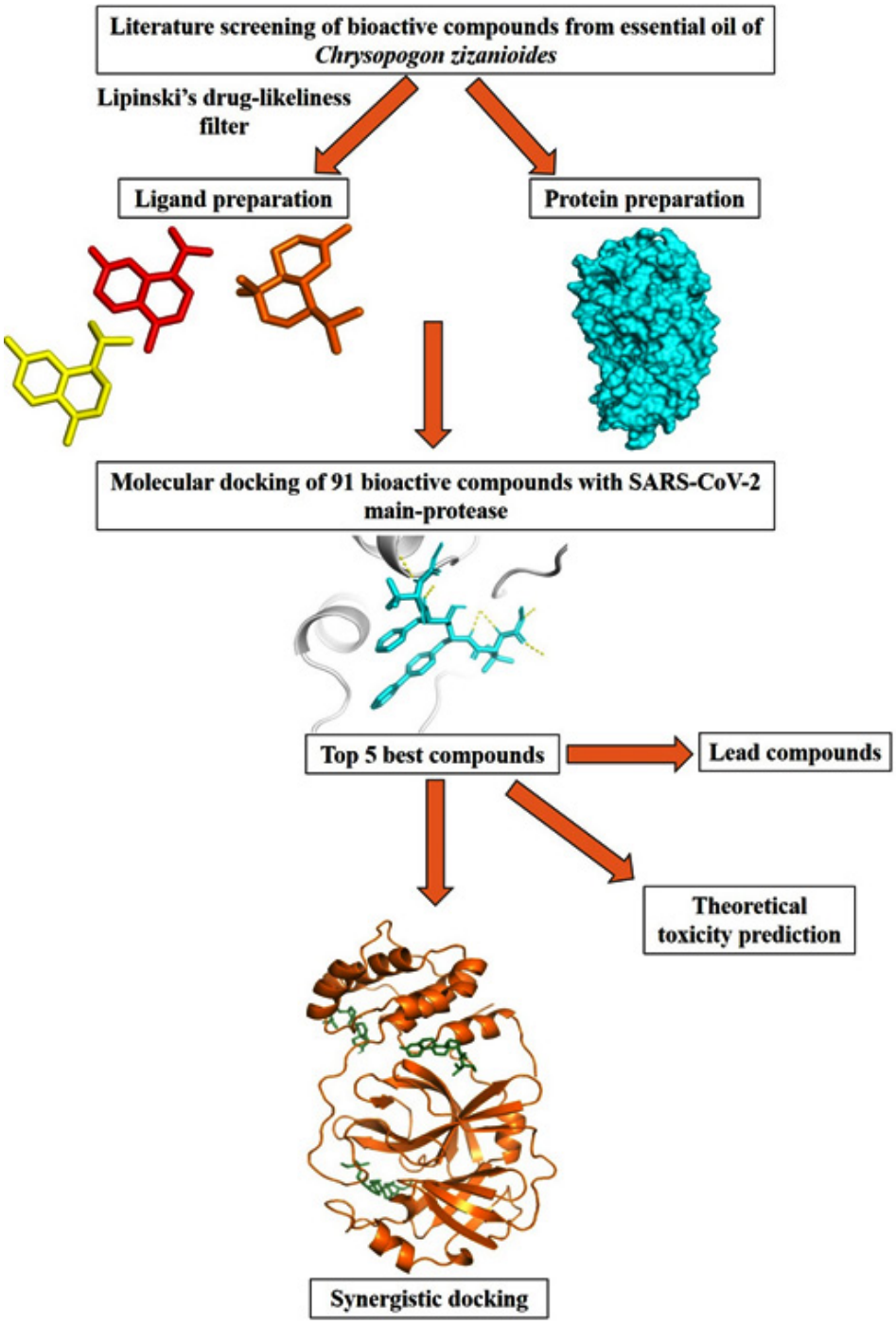

Fig. 1. Workflow of the research

Table 1. Binding energy of bioactive compounds against M^{pro}

S. No	Compound	Binding energy (kcal/mol)	Ki value
1	β-Sitosterol	-7.5	3.13 μM
2	Campesterol	-7.4	3.71 μM
3	Stigmast-4-en-3-one	-7.3	4.39 μM
4	β-Vatirenene	-6.7	12.1 μM
5	Stigmasterol	-6.7	12.1 μM
6	δ-Cadinene	-6.5	16.9 μM
7	Globulol	-6.4	20.1 μM
8	Guaiol	-6.4	20.1 μM
9	Isovalencenol	-6.4	20.1 μM
10	β-Caryophyllene oxide	-6.3	23.8 μM
11	Cedrylacetate	-6.3	23.8 μM
12	γ-Himachalene	-6.3	23.8 μM
13	Khusenicacid	-6.3	23.8 μM
14	Khusimone	-6.3	23.8 μM
15	Nootkatone	-6.3	23.8 μM
16	β-Caryophyllene	-6.2	28.2 μM
17	β-Eudesmol	-6.2	28.2 μM
18	β-Guaiene	-6.2	28.2 μM
19	β-Vetivenene	-6.2	28.2 μM
20	Cis-α-guaiene	-6.2	28.2 μM
21	Cyclocopacamphan-12-ol	-6.2	28.2 μM
22	Prezizaene	-6.2	28.2 μM
23	Valencene	-6.2	28.2 μM
24	Allo-Aromadendrene	-6.1	33.3 μM
25	β-Patchoulene	-6.1	33.3 μM
26	β-Vetivone	-6.1	33.3 μM
27	Cadina-1,4-diene(cubenene)	-6.1	33.3 μM
28	Cis-eudesm-6-en-11-ol	-6.1	33.3 μM
29	Isoledene	-6.1	33.3 μM
30	Isovalencenal	-6.1	33.3 μM
31	Spathulene	-6.1	33.3 μM
32	Vetiselinenol	-6.1	33.3 μM
33	α-Amorphene	-6.0	39.5 μM
34	α-Calacorene	-6.0	39.5 μM
35	α-Vetivone	-6.0	39.5 μM
36	α-Ylangene	-6.0	39.5 μM
37	β-Cadinene	-6.0	39.5 μM
38	β-Cedren-9-á-ol	-6.0	39.5 μM
39	β-Vetispirene	-6.0	39.5 μM
40	Cyclosativene	-6.0	39.5 μM
41	γ-Vetivenene	-6.0	39.5 μM
42	Khusimol	-6.0	39.5 μM
43	Zierone	-6.0	39.5 μM
44	Zizanoic acid	-6.0	39.5 μM
45	α-Eudesmol	-5.9	46.8 μM
46	α-Gurjunene	-5.9	46.8 μM
47	Aromadendrene epoxide	-5.9	46.8 μM
48	β-Humulene	-5.9	46.8 μM
49	β-Selinene	-5.9	46.8 μM
50	Bicyclovetivenol	-5.9	46.8 μM
51	Cedr-8-en-13-ol	-5.9	46.8 μM

52	Cis-eudesma-6,11-diene	-5.9	46.8 µM
53	δ-Amorphene	-5.9	46.8 µM
54	Dehydroaromadendrene	-5.9	46.8 µM
55	Deoxynivalenol	-5.9	46.8 µM
56	Eudesma-4,6-diene(δ-selinene)	-5.9	46.8 µM
57	Longifolene	-5.9	46.8 µM
58	Thujopsene	-5.9	46.8 µM
59	Ziza-6(13)-en-3-one	-5.9	46.8 µM
60	α-Copaene	-5.8	55.4 µM
61	α-Humulene	-5.8	55.4 µM
62	Caryophyllenyl alcohol	-5.8	55.4 µM
63	Eudesma-3,11-diene(α-selinene)	-5.8	55.4 µM
64	γ-Cadinene	-5.8	55.4 µM
65	γ-Muurolene	-5.8	55.4 µM
66	Isogermacrene D	-5.8	55.4 µM
67	Khusian-2-ol	-5.8	55.4 µM
68	Vetivenene	-5.8	55.4 µM
69	Viridiflorene	-5.8	55.4 µM
70	α-Cadinol	-5.7	65.6 µM
71	α-Curcumene	-5.7	65.6 µM
72	α-Muurolene	-5.7	65.6 µM
73	β-Lonol	-5.7	65.6 µM
74	Cycloisolongifolene	-5.7	65.6 µM
75	E-Caryophyllene	-5.7	65.6 µM
76	Khusimene	-5.7	65.6 µM
77	Khusinol	-5.7	65.6 µM
78	Valerenal	-5.7	65.6 µM
79	Valerenol	-5.7	65.6 µM
80	α-Nootkatol	-5.6	77.7 µM
81	Bisabolol	-5.6	77.7 µM
82	Cadina-4,9-diene	-5.6	77.7 µM
83	Cubenol	-5.6	77.7 µM
84	Farnesol	-5.6	77.7 µM
85	Isolongifolene	-5.6	77.7 µM
86	Khusol	-5.6	77.7 µM
87	Longifolenaldehyde	-5.6	77.7 µM
88	Sativene	-5.6	77.7 µM
89	Patchoulialcohol	-5.5	92.0 µM
90	Isoeugenol	-5.3	129 µM
91	β-Bisabolol	-4.0	1.16 mM

HIS164, MET49, MET165, THR25, THR45, and TYR54 amino acids in the active site cleft. The other supramolecular bonding interactions like non-covalent van der Waals, conventional hydrogen, alkyl, and ð-alkyl intermolecular interactions. One hydrogen bond was formed between the OH^- donor of Campesterol and oxygen acceptor of ASN142 at a distance of 2.5 Å. The compounds Stigmast-4-en-3-one (ÄG = -7.3 kcal/mol; Ki = 4.39 µM) > â-Vatirenene (ÄG = -6.7 kcal/mol; Ki = 12.1 µM) > Stigmasterol (ÄG = -6.7 kcal/mol; Ki = 12.1 µM) were ranked successively with decreasing inhibition potential. It is important to note that the compounds â-Sitosterol, Campesterol, and Stigmast-4-en-3-one outperformed the atazanavir's control drug. Atazanavir is one best protease inhibitors against several viral diseases. Atazanavir possessed an energy of -7.0 kcal/mol and Ki = 7.3 µM forming seven conventional hydrogens, ð-alkyl, van der Waals, and ð-sulphur interactions with protease (Figure 5).

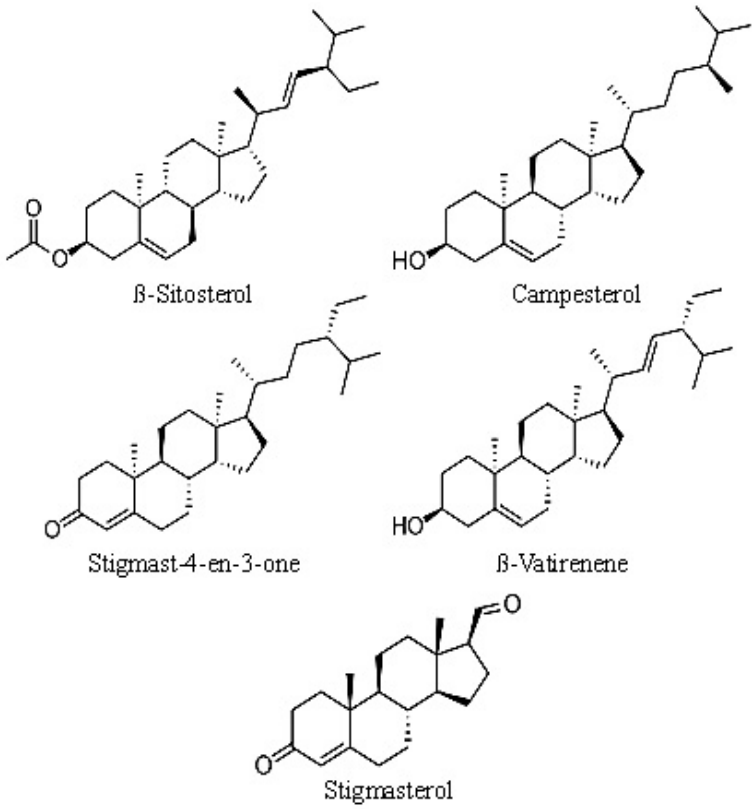

Fig. 2. Molecular structure of top ranked bioactive compounds

Thus, the bioactive compounds that showed greater potential than atazanavir were chosen for sequential synergistic docking. Synergism is defined as the cooperation of multiple agents or substances (here inhibitors) to display enhanced effects compared to the personal effect.

Sequential synergistic docking

Figure 6 shows the synergistic interaction of bioactive compounds with M^{pro}. The synergistic docking revealed promising results upon the interaction of multiple compounds. The docked â-Sitosterol-M^{pro} complex was kept constant and used as the enzyme; then, Campesterol and Stigmast-4-en-3-one were sequentially docked into the â-Sitosterol-M^{pro} complex. Initially, docking Campesterol onto the â-Sitosterol-M^{pro} complex did not significantly improve the free binding energy. However, upon docking Stigmast-4-en-3-one, the free binding energy reduced drastically from its initial -7.5 kcal/mol to -7.9 kcal/mol, which is a significant sign of inhibition more remarkable than their individual effects. The decrease in binding energy is attributed to the low entropy change as the bioactive compounds are hydrophobic in nature. The formation of hydrophobic supramolecular bonding interactions including van der Waals, hydrogen, alkyl, ð-alkyl, ð-sigma, and carbon-hydrogen was dominant (Table 3).

Moreover, no existing intermolecular bonds were broken or dislocated upon docking multiple compounds; thus, an improvement in binding energy was achieved. It is to be noted that Campesterol and Stigmast-4-en-3-one did not overlap on the â-Sitosterol in the active site; instead, they interacted with allosteric sites of M^{pro}, causing inhibition. Therefore, the combined effect of bioactive compounds showed augmented inhibition, and it is clear that the compounds have the potentials to be used for further studies to develop novel drug candidates. Muralidharan et al. performed similar synergistic docking of lopinavir, ritonavir, and oseltamivir against SARS-CoV-2

main-protease and obtained free binding energy of -8.3 kcal/mol, which is slightly lower than the present study [27]

Validation of docking procedure

The re-docked X77 ligand onto M^{pro} showed free binding energy of -8.3 kcal/mol (Figure 7). The re-docked protein-ligand complex was precisely bound to the active site and was superimposed onto the PDB co-crystal structure and an RMSD of 0.7 Å was obtained. The re-docked complex also interacted with the same amino acids as the actual co-crystal structure. The superimposition was done successfully with no atomic and stearic clashes between the complexes, which proved that the docking procedure was valid. Joshi et al. also reported a low RMSD (< 2.0 Å) [28].

Thus, the compounds from *Chrysopogon zizanioides* showed good antiviral potential by inhibiting the proteolytic activity of SARS-CoV-2 M^{pro} using computational approaches. This was accomplished by forming wide intermolecular supramolecular bonding between viral protease and bioactive compounds. The top compounds were sequentially docked into the protease and showed good binding potential. To validate the molecular docking, re-docking and superimposition were performed to validate the study. Alagu Lakshmi et al. studied the antiviral potential of a few essential compounds â-Sitosterol, Stigmasterol, â-Vetivenene, Vetivone, á-Cadinene, á-Calacorene from *Chrysopogon zizanioides* against SARS-CoV-2 M^{pro} (PDB Id: 5R82), human ACE2 recceptor (PDB Id: 1R42), and spike protein (PDB Id: 6VYB), and reported similar inhibition potentials compared to the present work [29]. Santra et al. studied the antiviral property of essential bioactive compounds from *Chrysopogon zizanioides* against the spike glycoprotein of SARS-CoV-2 and human ACE2 receptor and reported binding energies -8.0 to -7.1 kcal/mol, which closely resembles to the results reported in the present work. There has been no report on the simultaneous synergistic effect of *Chrysopogon zizanioides* against M^{pro} [30]. The top-ranked

Table 2. Interaction of bioactive compounds with M^{pro} (PDB Id: 6W63)

S. No	Compound	Binding energy (kcal/mol)	Interacting amino acid residues	No. of hydrogen bonds	Ki value
1	β-Sitosterol	-7.5	ARG188, ASN142, ASP187, CYS44, GLN189, GLN192, GLU166, GLY143, HIS41, MET49, MET165, THR25, THR26, THR190, TYR54	-	3.13 µM
2	Campesterol	-7.4	ARG188, ASN142, ASN187, CYS44, GLN189, GLU166, HIS41, HIS164, MET49, MET165, THR25, THR45, TYR54	1	3.71 µM
3	Stigmast-4-en-3-one	-7.3	ASN151, ASP153, ASP295, GLN107, GLN110, HIS246, ILE249, PHE294, PRO108, THR111, THR292, VAL202	1	4.39 µM
4	β-Vatirenene	-6.7	ARG188, ASP187, CYS44, GLN189, HIS41, HIS164, MET49, MET165, THR25, TYR54	-	12.1 µM
5	Stigmasterol	-6.7	ASN151, ASP153, ASP295, GLN107, GLN110, ILE106, LYS102, PHE294, SER158, THR111, THR292, VAL104	1	12.1 µM
6	Atazanavir*	-7.0	ALA285, ARG131, ASN238, ASP197, ASP289, LEU271, LEU272, LEU286, LEU287, LYS137, LYS236, MET276, THR198, THR199, TYR237, TYR239	7	7.3 µM

*- Control drug used in the present study

â-Sitosterol, plant-based cholesterol, is a medicinal herb commonly used in Chinese medicine showed promising potential as an antiviral agent against influenza A virus targeting the p38 mitogen-activated protein kinase pathway at 150 to 450 µM concentration [31]. â-Sitosterol isolated from *Isatis indigotica* roots inhibited SARS-CoV-1 3C-like protease under *in-vitro* [32]. Tsai et al. reported the promising inhibition potential of â-Sitosterol at low concentrations from methanolic *Strobilanthes cusia* leaf extracts against Human Coronavirus NL63 [33]. Oladele et al. reviewed the anti-COVID potential of â-Sitosterol, stigmasterol, campesterol, etc., from Nigerian medicinal plants with excellent inhibition potentials [34]. These pieces of evidence proved the antiviral potential of bioactive compounds from *Chrysopogon zizanioides* against COVID-19. Apart from essential oils, the antiviral potentials of various flavonoid polyphenols, alkaloids, saponins, tannins, terpenoids, etc., were studied [35–39]. No compounds possessed toxicity and carcinogenic properties predicted using SwissADME and admetSAR webservers (Table 4), thus are safe for consumption without any side effects. Bioactive

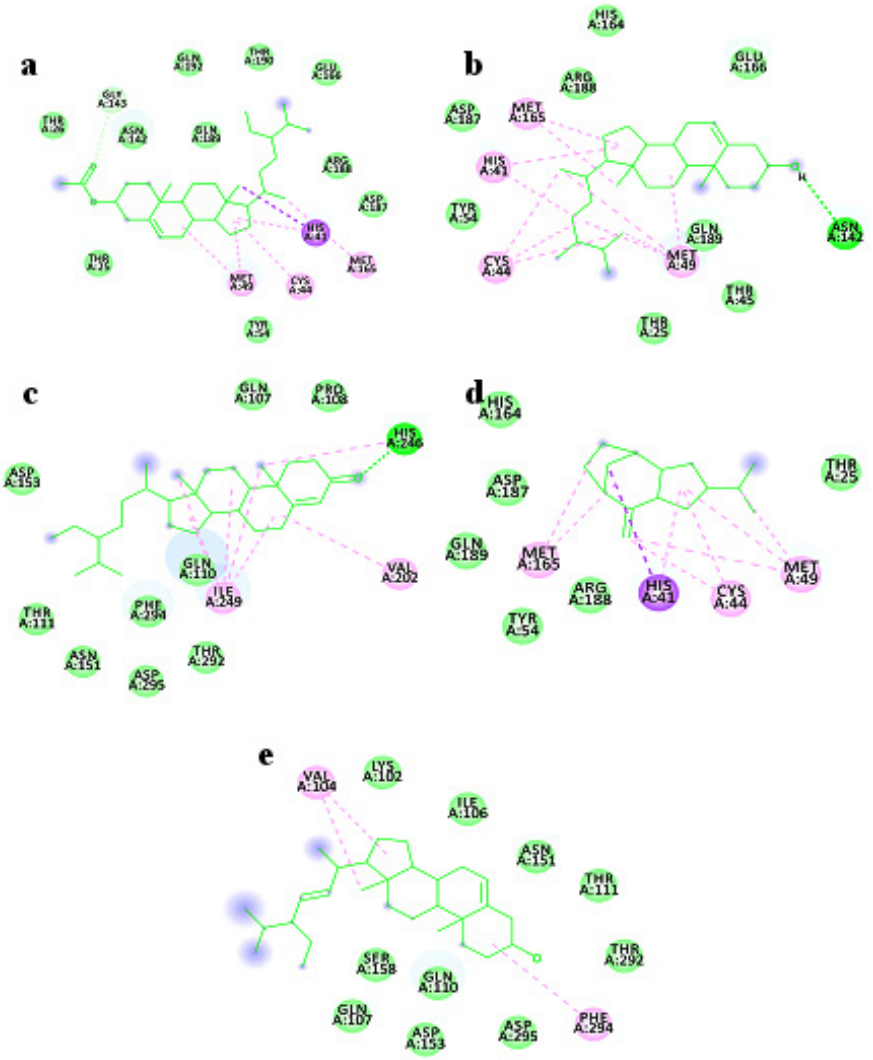

Fig. 3. Two-dimensional interaction map of top ranked compounds with M^{pro} a) β-Sitosterol; b) Campesterol; c) Stigmast-4-en-3-one; d) β-Vatirenene; e) Stigmasterol

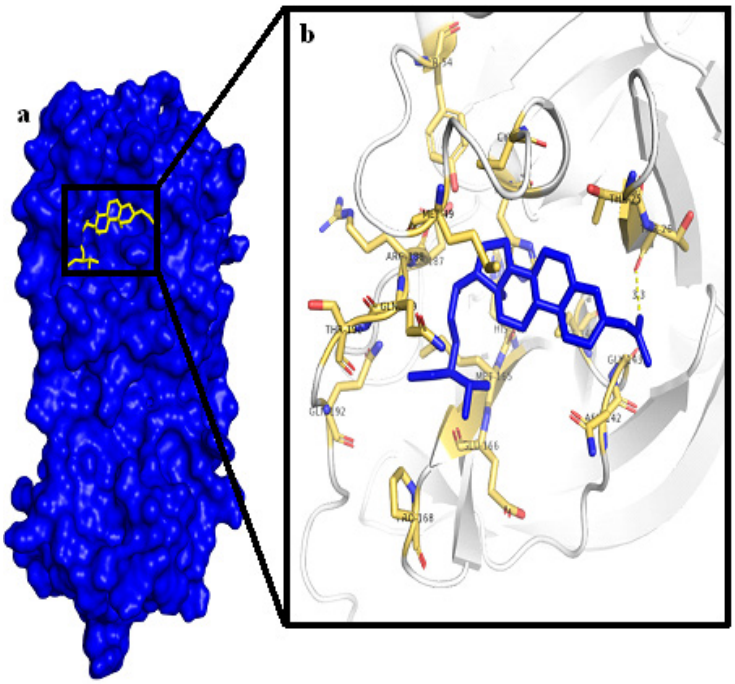

Fig. 4. Interaction of â-Sitosterol with M^{pro}: a) three-dimensional surface image; b) three-dimensional cartoon image

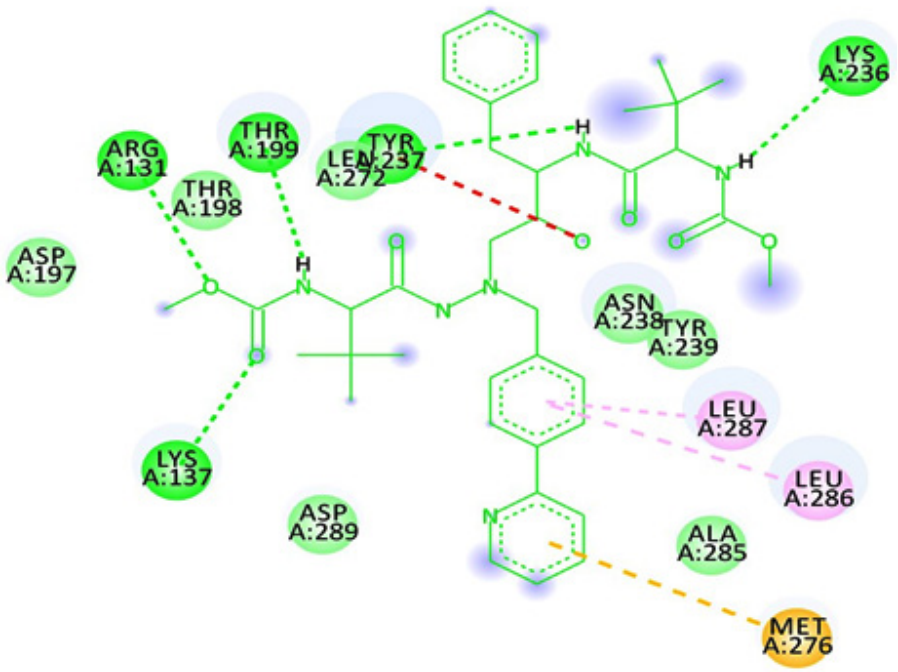

Fig. 5. Two-dimensional supramolecular bonding interaction of atazanavir with M^{pro}

compounds from the essential oils of *Chrysopogon zizanioides* have been reported to be non-genotoxic, non-hepatotoxic, and non-carcinogenic and are safe [40–44]. As the bioactive compounds possessed good binding energies with least toxicity, these compounds can be taken to next level of *in-vitro* studies.

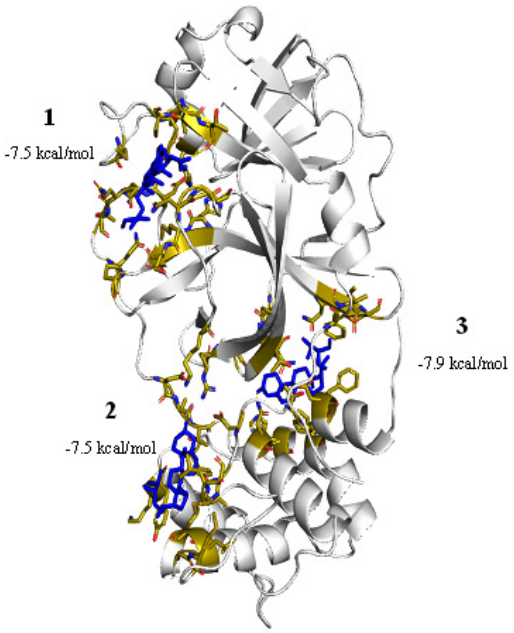

Fig. 6. Synergistic interaction of bioactive compounds against M^{pro}: 1) β-Sitosterol; 2) Campesterol; 3) Stigmast-4-en-3-one

SUMMARY AND CONCLUSIONS

Thus, the bioactive compounds from *Chrysopogon zizanioides* showed promising results towards the SARS-CoV-2 inhibition. Phytosterol â-Sitosterol displayed a free binding energy of -7.5 kcal/mol and Ki = 3.13 µM was found to be the most potent inhibitor against the

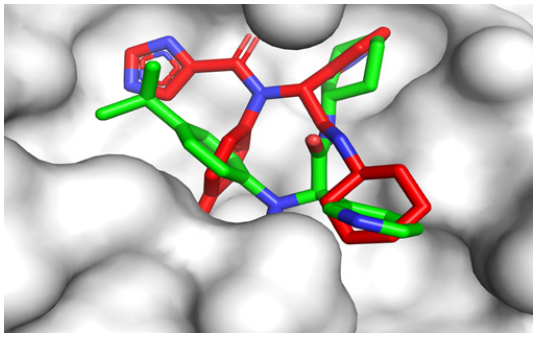

Fig. 7. Superimposed re-docked X77-M^{pro} (green) structure onto native co-crystal structure (red) from PDB (RMSD = 0.7 Å)

Table 3. Synergistic interaction of bioactive compounds with M^{pro}

S. No	Compound	Binding energy (kcal/mol)	Interacting amino acid residues	No. of hydrogen bonds
1	β-Sitosterol	-7.5	ARG188, ASN142, ASP187, CYS44, GLN189, GLN192, GLU166, GLY143, HIS41, MET49, MET165, THR25, THR26, THR190, TYR54	-
2	β-Sitosterol +Campesterol	-7.5	ARG131, ARG188, ASN142, ASN187, CYS44, GLN189, GLU166, HIS41, HIS164, LEU272, LEU286, LEU287, LYS137, MET49, MET165, THR25, THR45, THR199, TYR54, TYR237, TYR239	1
3	β-Sitosterol +Campesterol + Stigmast-4-en-3-one	-7.9	ARG131, ARG188, ASN142, ASN151, ASN187, ASP153, CYS44, GLN107, GLN110, GLN189, GLU166, HIS41, HIS164, HIS246, ILE249, LEU272, LEU286, LEU287, LYS137, MET49, MET165, PHE294, PRO108, THR25, THR45, THR111, THR199, TYR54, TYR237, TYR239, VAL202	1

Table 4. Predicted toxicity of top ranked bioactive compounds from *Chrysopogon zizanioides*

S. No	Bioactive compound	AMES toxicity	Carcinogens	Hepatotoxicity	Biodegradation	Acute oral toxicity (kg/mol)
1	β-Sitosterol	No	No	No	No	3.26
2	Campesterol	No	No	No	No	2.83
3	Stigmast-4-en-3-one	No	No	No	No	3.02
4	β-Vatirenene	No	No	No	No	1.86
5	Stigmasterol	No	No	No	No	3.38

M^{pro} of SARS-CoV-2 followed by Campesterol and Stigmast-4-en-3-one. The sequential synergistic inhibition of compounds was more effective than their individual potentials. The compounds were non-toxic and thus are safe for consumption. This study provides a road map for developing plant-based drugs. Future works will focus on *in-vitro* and further *in-vivo* clinical trials for developing herbal-based medicines against COVID-19.

ACKNOWLEDGEMENT

The authors sincerely thank Vels Institute of Science Technology and Advanced Studies, Chennai for the successful completion of research work.

Conflicts of interest

No conflicts of interest declared by the authors.

Funding sources

No specific grant was received from any funding agency to carry out the research work.

REFERENCES

1. Guo Y.R., Cao Q.D., Hong Z.S., Tan Y.Y., Chen S.D., Jin H.J., Tan K.S., Wang D.Y., Yan Y. The origin, transmission and clinical therapies on coronavirus disease 2019 (COVID-19) outbreak- An update on the status. *Mil. Med. Res.* 2020;7(1):1–10.
2. Sheahan T.P., Sims A.C., Leist S.R., Schäfer A., Won J., Brown A.J., Montgomery S.A., Hogg A., Babusis D., Clarke M.O., Spahn J.E. Comparative therapeutic efficacy of remdesivir and combination lopinavir, ritonavir, and interferon beta against MERS-CoV. *Nat. Commun*. 2020;11(1):1–14.
3. Xue X., Yu H., Yang H., Xue F, Wu Z., Shen W., Li J., Zhou Z., Ding Y., Zhao Q., Zhang X.C. Structures of Two Coronavirus Main Proteases: Implications for Substrate Binding and Antiviral Drug Design. *J. Virol*. 2008;82(5):2515–2527.
4. Rates S. M. K. Plants as source of drugs. *Toxicon*. 2001;39(5):603–613.
5. Pripdeevech P., Wongpornchai S., Promsiri A. Highly volatile constituents of Vetiveria zizanioides roots grown under different cultivation conditions. *Molecules*. 2006; 11(10):817–826.
6. Jaiswal Y.S., Williams L.L. A glimpse of Ayurveda – The forgotten history and principles of Indian traditional medicine. *J. Tradit. Complement. Med*. 2017;7(1):50–53.
7. Varaha surya P.D., Chauhan S.S., Tyagi S. A Review on Vetiveria zizanioides Species. *Research & Reviews: Journal of Herbal Science*. 2020;9(3):1–3.
8. Meng X.Y., Zhang H.X., Mezei M., Cui M. Molecular Docking: A Powerful Approach for Structure-Based Drug Discovery. *Curr. Comput.-Aided Drug Des.* 2012;7:146–157.
9. Martinez J., Rosa P.T.V., Menut C., Leydet A., Brat P., Pallet D., Meireles M.A. Valorization of brazilian vetiver (Vetiveria zizanioides (L.) Nash ex Small) oil. *J. Agric. Food Chem*. 2004;52(21):6578–6584.
10. David A., Wang F., Sun X., Li H., Lin J., Li P., Deng G. Chemical Composition, Antioxidant, and Antimicrobial Activities of Vetiveria zizanioides (L.) Nash Essential Oil Extracted by Carbon Dioxide Expanded Ethanol. *Molecules*. 2019;24(10):1897.
11. Lipinski C.A. Lead-and drug-like compounds: The rule-of-five revolution. *Drug Discov. Today Technol*. 2004;1(4):337–341.
12. O'Boyle N.M., Banck M., James C.A., Morley C., Vandermeersch T., Hutchison G.R. Open Babel: An Open chemical toolbox. *J. Cheminform*. 2011; 3(1):1–14.
13. Hartree D.R. The Wave Mechanics of an Atom with a Non-Coulomb Central Field Part II Some Results and Discussion. *Math. Proc. Camb.*

Philos. Soc. 1928;24(1):111–132.
14. Martinez J.P., The Hartree-Fock method: from self-consistency to correct symmetry. *Annalen der Physik*. 2017;529(1-2):1600328.
15. Guex N., Peitsch M.C., SWISS-MODEL and the Swiss-PdbViewer: An environment for comparative protein modelling. *Electrophoresis*. 1997;18(15):2714–2723.
16. Bonvin A.M.J.J., Mark A.E., van Gunsteren, W.F. GROMOS96 benchmarks for molecular simulation. *Comput. Phys. Commun*. 2000;128(3):550–557.
17. Zhang Z., Li Y., Lin B., Schroeder M., Huang B. Identification of cavities on protein surface using multiple computational approaches for drug binding site prediction. *Bioinformatics*. 2011;27(15):2083–2088.
18. Pant S., Singh M., Ravichandiran V., Murty U.S.N., Srivastava H.K. Peptide-like and small-molecule inhibitors against Covid-19. *J. Biomol. Struct. Dyn*. 2020;39(8):2904–2913.
19. Trott O., Olson A.J. AutoDock Vina: Improving the speed and accuracy of docking with a new scoring function, efficient optimization, and multithreading. *J. Comput. Chem*. 2009;31(2):455–461.
20. Morris G.M., Ruth H., Lindstrom W., Sanner M.F., Belew R.K., Goodsell D.S., Olson A.J. AutoDock4 and AutoDockTools4: Automated docking with selective receptor flexibility. *J. Comput. Chem*. 2009;30(16):2785–2791.
21. C S., S D.K., Ragunathan V., Tiwari P., A S., Brindha Devi B.D. Molecular docking, validation, dynamics simulations, and pharmacokinetic prediction of natural compounds against the SARS-CoV-2 main-protease. *J. Biomol. Struct. Dyn.* 2020;40(2):585–611.
22. Daina A., Michielin O., Zoete V. SwissADME: A free web tool to evaluate pharmacokinetics, drug-likeness and medicinal chemistry friendliness of small molecules. *Sci. Rep*. 2017;7(1):1–13.
23. Yang H., Lou C., Sun L., Li J., Cai Y., Wang Z., Li W., Liu G., Tang Y. AdmetSAR 2.0: Web-service for prediction and optimization of chemical ADMET properties. *Bioinformatics*. 2019;35(6):1067–1069.
24. Asadbeigi M., Mohammadi T., Rafieian-Kopaei M., Saki K., Bahmani M., Delfan M., Traditional effects of medicinal plants in the treatment of respiratory diseases and disorders: An ethnobotanical study in the Urmia. *Asian Pac. J. Trop. Med*. 2014;7:S364–S368.
25. Peng H.Y., Lai C.C., Lin C.C., Chou S.T. Effect of Vetiveria zizanioides essential oil on melanogenesis in melanoma cells: Downregulation of tyrosinase expression and suppression of oxidative stress. *Sci. World J*. 2014,2014:213013.
26. Lavanya P., Ramaiah S., Anbarasu A. Ethyl 4-(4-methylphenyl)-4-pentenoate from Vetiveria zizanioides Inhibits Dengue NS2B–NS3 Protease and Prevents Viral Assembly: A Computational Molecular Dynamics and Docking Study. *Cell Biochem. Biophys*. 2016;74(3):337–351.
27. Muralidharan N., Sakthivel R., Velmurugan D., Gromiha M.M. Computational studies of drug repurposing and synergism of lopinavir, oseltamivir and ritonavir binding with SARS-CoV-2 protease against COVID-19. *J. Biomol. Struct. Dyn*. 2021;39(7):2673–2678.
28. Joshi T., Sharma P., Joshi T., Pundir H., Mathpal S., Chandra S. Structure-based screening of novel lichen compounds against SARS Coronavirus main protease (Mpro) as potentials inhibitors of COVID-19. *Mol. Divers*. 2020;25(3):1665–1677.
29. Alagu Lakshmi S., Shafreen R.M.B., Priya A., Shunmugiah, K.P. Ethnomedicines of Indian origin for combating COVID-19 infection by hampering the viral replication: using structure-based drug discovery approach. *J. Biomol. Struct. Dyn*. 2020;39(13):4594–4609.
30. Santra S., Das S.G., Halder S.K., Kuntal G. Structure-based assortment of herbal analogues against spike protein to restrict COVID-19 entry through hACE2 receptor: An in-silico approach. *Acta Biol. Szeged*. 2020;64:159–171.
31. Zhou B.X., Li, J., Liang, X.L., Pan X.P., Hao Y.B., Xie P.F., Jiang H.M., Yang Z.F., Zhong N.S. â-sitosterol ameliorates influenza A virus-induced proinflammatory response and acute lung injury in mice by disrupting the cross-talk between RIG-I and IFN/STAT signaling. *Acta Pharmacol. Sin*. 2020;41(9):1178–1196.
32. Lin C.W., Tsai F.J., Tsai C.H., Lai C.C., Wan L., Ho T.Y., Hsieh C.C., Chao P.D. Anti-SARS coronavirus 3C-like protease effects of Isatis indigotica root and plant-derived phenolic compounds. *Antiviral Res*. 2005;68(1):36–42.
33. Tsai Y.C., Lee C.L., Yen H.R., Chang Y.S., Lin Y.P., Huang S.H., Lin C.W. Antiviral action of tryptanthrin isolated from strobilanthes cusia leaf against human coronavirus NL63. *Biomolecules*. 2020;10(3):366.
34. Oladele J.O., Ajayi E.I., Oyeleke O.M., Oladele O.T., Olowookere B.D., Adeniyi B.M., Oyewole O.I., Oladiji A.T. A systematic review on COVID-19 pandemic with special emphasis on curative potentials of Nigeria based medicinal plants. *Heliyon*. 2020;6(9):e04897.
35. Liskova A., Samec M., Koklesova L., Samuel S.M., Zhai K., Al-Ishaq R.K., Abotaleb M., Nosal V., Kajo K., Ashrafizadeh M., Zarrabi A.

Flavonoids against the SARS-CoV-2 induced inflammatory storm. *Biomed. Pharmacother*. 2021;138:111430.

36. Falade V.A., Adelusi T.I., Adedotun, I.O., Abdul-Hammed, M., Lawal, T.A., Agboluaje S.A. In silico investigation of saponins and tannins as potential inhibitors of SARS-CoV-2 main protease (Mpro). *In Silico Pharmacol*. 2021;9(1):9.
37. Wen C.C., Kuo Y.H., Jan J.T., Liang P.H., Wang S.Y., Liu H.G., Lee C.K., Chang S.T., Kuo C.J., Lee S.S., Hou C.C. Specific plant terpenoids and lignoids possess potent antiviral activities against severe acute respiratory syndrome coronavirus. *J. Med. Chem*. 2007;50(17):4087–4095.
38. Alrasheid A.A., Babiker M.Y., Awad T.A. Evaluation of certain medicinal plants compounds as new potential inhibitors of novel corona virus (COVID-19) using molecular docking analysis. *In Silico Pharmacol*. 2021;9:10.
39. Ismail E.M.O.A., Shantier S.W., Mohammed M.S., Musa H.H., Osman W., Mothana, R.A. Quinoline and quinazoline alkaloids against Covid-19: An in silico multitarget approach. *J. Chem*. 2021;2021:3613268.
40. Paniagua-Pérez R., Madrigal-Bujaidar E., Reyes-Cadena S., Molina-Jasso D., Gallaga J.P., Silva-Miranda A., Velazco O., Hernández N., Chamorro G. Genotoxic and cytotoxic studies of beta-sitosterol and pteropodine in mouse. *Journal of Biomedicine and Biotechnology*. 2005;2005:129127.
41. Alexander-Lindo R.L., Morrison E.Y.S.A. Nair M.G. Hypoglycaemic effect of stigmast-4-en-3-one and its corresponding alcohol from the bark of Anacardium occidentale (cashew). *Phytother. Res*. 2004;18(5):403–407.
42. O'Callaghan Y., Kenny O., O'Connell N.M., Maguire A.R., McCarthy F.O., O'Brien, N.M. Synthesis and assessment of the relative toxicity of the oxidised derivatives of campesterol and dihydrobrassicasterol in U937 and HepG2 cells. *Biochimie.* 2013;95(3):496–503.
43. Scientific Opinion on the safety of stigmasterol-rich plant sterols as food additive. *EFSA Journal*. 2012;10(7):2760.
44. Tao C., Shkumatov A.A., Alexander S.T., Ason, B.L., Zhou M. Stigmasterol accumulation causes cardiac injury and promotes mortality. *Commun. Biol*. 2019;2(1):20.